RF MIM Capacitors Using High-K Al_2O_3 and $AlTiO_x$ Dielectrics

S. B. Chen, C. H. Lai, Albert Chin, J. C. Hsieh*, and J. Liu*

Dept. of Electronics Eng., National Chiao Tung Univ., Hsinchu, Taiwan
*United Microelectronics Cooperation, Hsinchu, Taiwan

Abstract — **Record high capacitance density of 0.5 and 1.0 $\mu F/cm^2$ are obtained for Al_2O_3 and $AlTiO_x$ MIM capacitors respectively, with loss tangent < 0.01 and process compatible to existing VLSI back-end integration. However, the $AlTiO_x$ MIM capacitor has large capacitance reduction as increasing frequencies. In contrast, the Al_2O_3 MIM capacitor has good device integrity of low leakage current of 4.3×10^{-8} A/cm^2, small frequency-dependent capacitance reduction, and good reliability.**

I. Introduction

RF MIM capacitor is one of the important devices for MMIC that is widely used for impedance matching and filtering. However, the area of total capacitors usually occupies a large portion of the whole ICs, because of the required relatively large capacitance value (a few pF) in MMICs and the small capacitance/area. Therefore, it is highly desirable to increase the capacitance per unit area. Besides, other capacitor requirements of low DC leakage current, small frequency dependent capacitance, low loss tangent, and high reliability should also be satisfied simultaneously. To achieve this goal, it is necessary to apply high dielectric-constant (k) dielectrics for RF MIM capacitors because the capacitance density is $\varepsilon_0 k/t_d$ and reducing dielectric thickness t_d usually generates undesired high leakage current and loss tangent. Recently, we have published high-k Al_2O_3 and La_2O_3 dielectrics for possible replacing conventional SiO_2 in the gate capacitor of MOSFET [1]-[4]. Several times larger k value than conventional SiO_2 (k=3.9) has been reported and at the same time achieves good gate dielectric integrity. However, the fabrication of high-k MIM capacitors faces the additional challenge from VLSI process integration: the maximum temperature of forming high-k MIM capacitor should not excess 400°C for back-end process integration [5]. In this paper, we report the application of high-k Al_2O_3 and $AlTiO_x$ for RF MIM capacitors. The advantage of $AlTiO_x$ capacitor [3] is the increased k value by adding Ti into Al-O because very high-k of 86 has been reported in TiO_2 [6]. Very large capacitance density of 0.5 and 1.0 $\mu F/cm^2$ are measured for Al_2O_3 and $AlTiO_x$ MIM capacitors respectively, which is the highest capacitance density reported in literature [7]-[8]. However, significant capacitance reduction at high frequency is observed for $AlTiO_x$ MIM capacitors. In sharp contrast, the Al_2O_3 MIM capacitor has good integrity of low DC leakage current, small capacitance reduction, low loss tangent, and high reliability that can minimize the size of MMIC substantially and satisfies the VLSI integration requirement.

II. Experimental Procedure

The MIM capacitors were fabricated using 4-in p-type Si with resistivity of 5-10 Ω-cm. Additional 5000 Å thermal oxide was first grown for VLSI back-end process integration. Then coplanar transmission lines [9]-[10] with GSG probe were fabricated on oxide-isolated Si substrates using deposited Pt/Ti bi-layer followed by subsequent patterning. The transmission line also serves as both top and bottom electrodes of MIM capacitor. Then thin Al or Ti/Al was deposited under high vacuum condition on patterned bottom Al transmission line, followed by subsequent oxidation and annealing to form respective high-k Al_2O_3 or $AlTiO_x$ [1]-[4]. The oxidation was performed only using dry O_2 because of the strong reaction between oxygen and Al or Ti. However, the maximum temperature is kept only at 400°C for VLSI process integration consideration. Finally, Al is deposited and patterned for both top capacitor electrode and transmission line, and the device area is 50 μm×50 μm. The Al_2O_3 and $AlTiO_x$ capacitors were measured using HP4284A precision LCR meter at 100 KHz and 1 MHz [3], while the S-parameters were measured by HP8510C network analyzer ranging from 200 MHz to 20 GHz [9]-[10]. The measured S-parameters are de-embedded from a dummy device [9]-[10] and the high frequency capacitance plus resistance values are extracted using an equivalent circuit model shown in Fig. 4.

III. Results and Discussion

A. Low Frequencies Characteristics

Fig. 1 depicts the C-V characteristics of Al_2O_3 MIM capacitors at different frequencies, and a large capacitance

0-7803-7239-5/02/$10.00 © 2002 IEEE

per unit area of 0.5 μF/cm^2 is measured. It can be seen that no obvious reduction of capacitance is observed for frequencies ranging from 100 KHz to 1 MHz, which indicates the excellent qualities of Al_2O_3 MIM capacitor at intermediate frequency region.

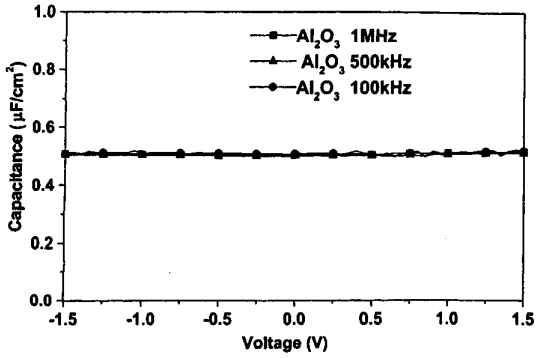

Fig. 1. C-V characteristics of the Al_2O_3 MIM capacitors measured at the frequencies of 100 KHz, 500 KHz and 1 MHz. Negligible capacitance reduction can be observed for increasing frequency from 100 KHz to 1 MHz.

Fig. 2 shows the C-V characteristics of $AlTiO_x$ MIM capacitors at different frequencies, and a very large capacitance per unit area of ~1.0 μF/cm^2 is measured at 100KHz. However, severe capacitance reduction can be observed in $AlTiO_x$ even increasing frequency to 1 MHz. Although $AlTiO_x$ capacitor exhibits higher capacitance and dielectric constant than Al_2O_3, this merit is almost compensated by the capacitance reduction phenomena at 1MHz.

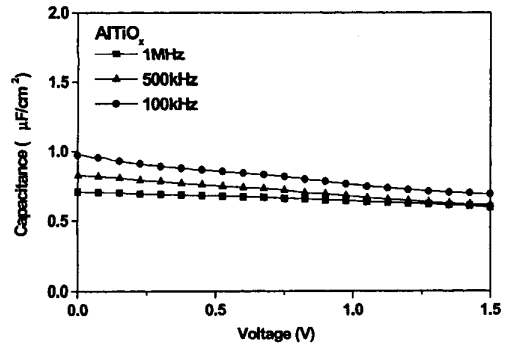

Fig. 2. C-V characteristics of the $AlTiO_x$ capacitors measured at the frequencies of 100 KHz and 1 MHz. Very large capacitance reduction is found from 100 KHz to 1 MHz.

Figs. 3(a) and 3(b) shows the J-V characteristics of Al_2O_3 and $AlTiO_x$ MIM capacitors before and after constant voltage stress, respectively. As shown in Fig. 3, the leakage current in Al_2O_3 MIM capacitor is only 4.3×10^{-8} A/cm^2 which is much smaller than that in $AlTiO_x$ MIM capacitor. It is noted that the physical thickness of Al_2O_3 and $AlTiO_x$ are the same of 120 Å. The relatively larger leakage current in $AlTiO_x$ capacitor than in Al_2O_3 capacitor may be due to both smaller bandgap and weaker bond related higher defects in Ti-O. This is further confirmed by the larger magnitude of stress-induced leakage current (SILC) in $AlTiO_x$ capacitor than that in Al_2O_3 capacitor. The small amount of current increase after stress in Al_2O_3 MIM capacitor suggests the excellent reliability. The relatively large leakage current of $AlTiO_x$ MIM capacitor as compared with the $AlTiO_x$ MIS gate capacitor on Si [4] may be due to the limited annealing temperature in MIM case because of the VLSI process integration constraint.

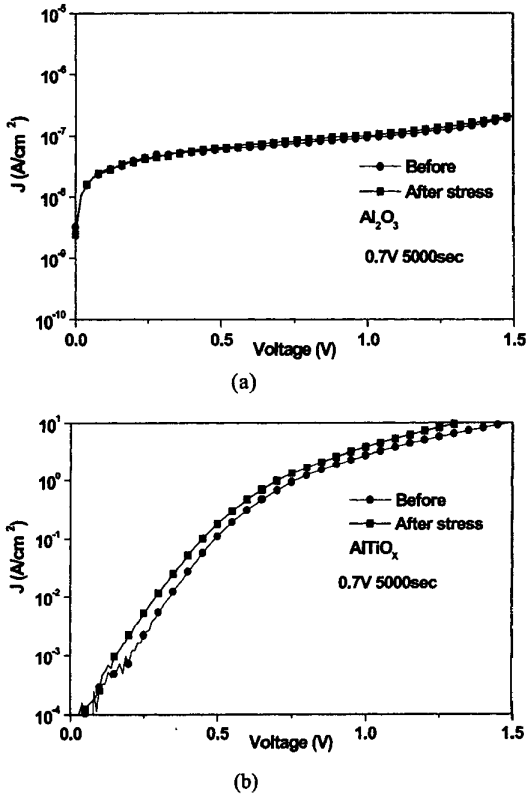

Fig. 3. J-V characteristics of (a) Al_2O_3 and (b) $AlTiO_x$ MIM capacitors before and after stress. The small change of leakage current in Al_2O_3 MIM capacitor after stress suggests the excellent reliability.

B. High Frequencies Characteristics

To investigate the capacitor characteristics of these two dielectrics at RF regime, we have first established the equivalent circuit model for capacitance and loss tangent extraction. As shown in Fig. 4, the shunt C and G are the basic models for high-k capacitor, whereas additional small series R and L represent the parasitic resistance and inductance in the coplanar transmission line used for RF measurements. Notice that the shunt G is originated from the gate dielectric leakage current; in another word, the gate dielectric having higher leakage current will produce larger loss tangent and power dissipation.

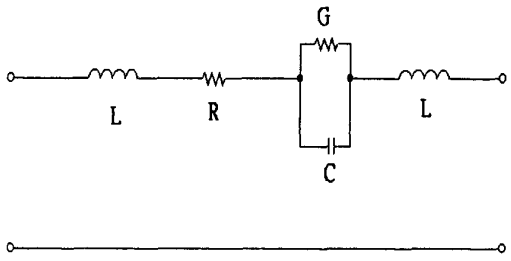

Fig. 4. The equivalent circuit model for capacitor simulation at RF regime.

Figs. 5(a) and 5(b) illustrate the measured S-parameters for Al_2O_3 and $AlTiO_x$ MIM capacitors, respectively. For comparison, the simulated results using equivalent circuit model in Fig. 4 are also shown in these figures. The good agreement between measured and simulated data over the wide frequency range from 200 MHz to 20 GHz suggests that the equivalent circuit model shown in Fig. 4 is suitable and reliable for capacitor extraction.

We have further plotted the extracted capacitance from the measured and simulated C-V data and s-parameters shown in previous figures. Fig. 6 demonstrates the frequency-dependent capacitance reduction for Al_2O_3 and $AlTiO_x$ MIM capacitors. Only a small amount of capacitance reduction for Al_2O_3 MIM capacitor is found over the entire frequency range from 100 KHz to 20 GHz. In sharp contrast, very large capacitance reduction is observed for $AlTiO_x$ MIM capacitor and the capacitance value gradually reduces to the same value as that of Al_2O_3 MIM capacitor. The reason why $AlTiO_x$ MIM capacitor exhibits severe capacitance reduction may be due to the weak bonded Ti-O_x and is dependent on the process and microstructure. The weak bonded Ti-O_x can generate high defect density at low annealing temperature and may be responsible to the large capacitance reduction in $AlTiO_x$ MIM capacitor.

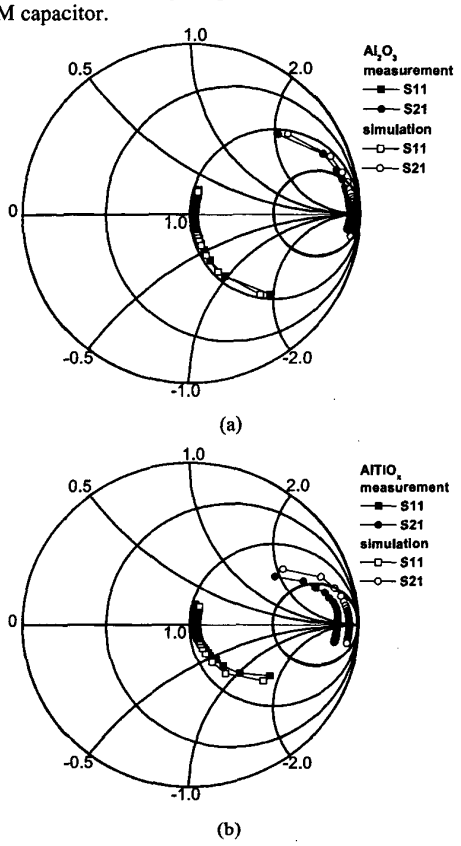

Fig. 5. The measured and simulated scattering parameters of (a) Al_2O_3 and (b) $AlTiO_x$ capacitors.

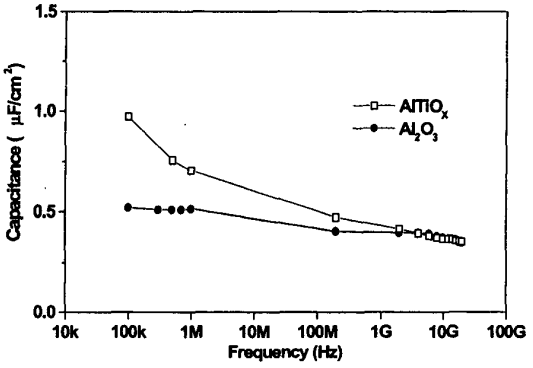

Fig. 6. The frequency-dependent capacitance for Al_2O_3 and $AlTiO_x$ MIM capacitors. Very large capacitance reduction in

$AlTiO_x$ MIM capacitor may be defect related because of the weak Ti-O_x band and low process temperature.

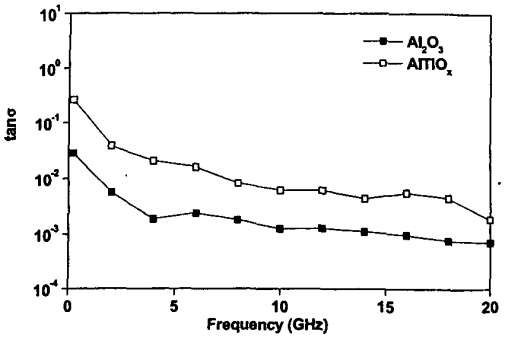

Fig. 7. The frequency-dependent loss tangent for Al_2O_3 and $AlTiO_x$ MIM capacitors. The small loss tangent less than 0.01 suggests the good capacitor performance.

We have also plotted the loss tangent from the measured and simulated C-V and s-parameters. Fig. 7 shows the loss tangent for Al_2O_3 and $AlTiO_x$ MIM capacitors. Good RF performance can be evidenced from the low loss tangent for Al_2O_3 and $AlTiO_x$ capacitors. However, the loss tangent for $AlTiO_x$ capacitor is near one order of magnitude higher than that for Al_2O_3 capacitor because of the larger leakage current in the $AlTiO_x$ capacitor.

IV. Conclusion

To reduce the chip size effectively, it is necessary to reduce the MIM capacitance substantially utilizing thin and high-k dielectrics. Record high capacitance density of 0.5 and 1.0 $\mu F/cm^2$ are obtained for Al_2O_3 and $AlTiO_x$ MIM capacitors respectively, but the $AlTiO_x$ MIM capacitor has large capacitance reduction as increasing frequencies. Besides the high capacitance density, the Al_2O_3 MIM capacitor exhibits low leakage current of 4.3×10^{-8} A/cm^2, low capacitance reduction rate, low loss tangent. The maximum process temperature of 400°C makes this technology compatible to current VLSI back-end process.

Acknowledgement

The authors would like to thank Y. M. Deng, K. M. Chen, and Dr. G. W. Huang at National Nano Devices Lab (NDL) for their help in the measurement. This work has been supported by NSC (90-2215-E-009-052) and UMC.

References

[1] A. Chin, C. C. Liao, C. H. Lu, W. J. Chen, and C. Tsai, "Device and Reliability of High-K Al_2O_3 gate dielectric with good mobility and low D_{it}," *Symp. on VLSI Technology*, pp. 133-134, June 1999.

[2] A. Chin, Y. H. Wu, S. B. Chen, C. C. Liao, and W. J. Chen, "High Quality La_2O_3 and Al_2O_3 Gate Dielectrics with Equivalent Oxide Thickness 5-10Å," *Symp. on VLSI Technology*, pp. 16-17, June 2000.

[3] M. Y. Yang, S. B. Chen, A. Chin, C. L. Sun, B. C. Lan, and S. Y. Chen, "One-Transistor PZT/Al_2O_3, SBT/Al_2O_3 and BLT/Al_2O_3 Stacked Gate Memory," *Int. Electron Devices Meeting (IEDM)*, Washington DC, USA, Dec. 2001.

[4] A. Chin, S. B. Chen, K. T. Chan, J. C. Hsieh, M. H. Chang, C. C. Lin, and J. Liu, "RF Performance Limitation of High-k $AlTiO_x$ and Al_2O_3 Gate Dielectrics," *Int. Workshop on Gate Insulator*, pp. 62-63, Tokyo, Japan, Nov. 2001.

[5] Y. H. Wu, A. Chin, K. H. Shih, C. C. Wu, C. P. Liao, S. C. Pai, C. C. Chi, "The fabrication of very high resistivity Si with low loss and cross talk," *IEEE Electron Device Lett.* 21, pp. 394-396, 2000.

[6] S. A. Campbell, D. C. Gilmer, X. C. Wang, M. T Hsieh, H. S. Kim, W. L. Gladfelter, and T. Yyan, "MOSFET transistors fabricated with high permitivity TiO_2 dielectrics," *IEEE Trans. Electron Devices*, vol. 44, no. 1, pp. 104-109, 1997.

[7] C. P. Yue and S. S. Wong, "A study on substrate effects of Silicon-based RF passive components," *IEEE MTT-S Intl. Microwave Symp. Dig.*, pp. 1625-1628, June 1999.

[8] P. Zurcher, P. Alluri, P. Chu, A. Duvallet, C. Happ, R. Henderson, J. Mendonca, M. Kim, M. Raymond, T. Remmel, D. Roberts, B. Steimle, J. Stipanuk, S. Straub, T. Sparks, M. Tarabbia, H. Thibieroz, and M. Miller, "Integration of thin film MIM capacitors and resistors into copper metallization based RF-CMOS and Bi-CMOS technologies," in *Int. Electron Devices Meeting (IEDM) Tech. Dig.*, pp. 153-156, Dec. 2000.

[9] K. T. Chan, A. Chin, C. M. Kwei, D. T. Shien, and W. J. Lin, "Transmission line noise from standard and proton-implanted Si," in *IEEE MTT-S Intl. Microwave Symp. Dig.*, pp. 763-766, June 2001.

[10] Y. H. Wu, A. Chin, K. H. Shih, C. C. Wu, C. P. Liao, S. C. Pai, and C. C. Chi, "RF loss and crosstalk on extremely high resistivity (10k-1MΩ-cm) Si fabricated by ion implantation," in *IEEE MTT-S Intl. Microwave Symp. Dig.*, pp. 221-224, June 2000.